

# AUTOMATIC DTM GENERATION FROM LASER-SCANNING DATA IN RESIDENTIAL HILLY AREA

Hossein Arefi<sup>(a)</sup>, Johannes Engels<sup>(a)</sup>, Michael Hahn<sup>(a)</sup> and Helmut Mayer<sup>(b)</sup>

<sup>(a)</sup> Department of Geomatics, Computer Sciences and Mathematics  
University of Applied Sciences, D-70174 Stuttgart, Germany  
{hossein.arefi, johannes.engels, michael.hahn}@hft-stuttgart.de

<sup>(b)</sup> Institute for Photogrammetry and Cartography  
Bundeswehr University Munich, D-85577 Neubiberg, Germany  
helmut.mayer@unibw.de

## Commission IV/4

**KEY WORDS:** LIDAR, Geodesic dilation, image reconstruction, digital terrain model, digital surface model, local range variation

## ABSTRACT:

Airborne laser scanning systems provide high quality 3D point clouds from the earth's surface. A Digital Surface Model (DSM) is provided from the LIDAR data after removing the outliers from the point clouds. Generating Digital Terrain Models (DTM) is one of the most important applications of the LIDAR data. During the past few years many methods have been proposed for DTM generation from LIDAR DSM data. Almost all of them work properly in smooth and non-undulated urban areas. Problems appear especially in hilly urban areas where the 3D objects (e.g. buildings) are situated on and around hills. In such areas it happens frequently that the height of the ground at one side of a building is much different from the height at the other side. Another problem is the discrimination of tops of steep hills from buildings situated on these hilltops. In this paper an approach based on geodesic morphological reconstruction (Arefi and Hahn, 2005) is proposed. The experimental investigation shows the potential and reliability of this algorithm.

## 1 INTRODUCTION

Airborne LIDAR data has become an acknowledged data source for the acquisition of precise digital surface models (DSM). In many applications the LIDAR DSM is used as a starting point to separate terrain and off-terrain regions and to produce digital terrain models (DTM) in this way. The process returns a normalized digital surface model (nDSM) as well which is complementary to the DSM. Various techniques and filtering methods have been proposed to generate DTMs from LIDAR data. Some first ideas were proposed in an early work on LIDAR data recorded in wooded areas based on the morphological opening operation (Kilian et al., 1996). (Kraus and Pfeifer, 1998) introduced another approach based on iterative linear prediction. They start with an approximate ground surface. Then a weight is defined to the data based on the distances from the ground surface to the measured points. If the height residual within surface interpolation is above a certain threshold, the corresponding point is classified as an off-terrain point and eliminated from the surface interpolation.

(Axelsson, 2000) (see also (Sithole and Vosselman, 2003)) described a method for DTM generation based on progressive densification of a triangular irregular network (TIN). The lowest points in large grids are selected as approximate ground points and a TIN is defined based on the selected points. In every iteration some new points are added to the TIN surface if they are below the threshold. The criterion for this assessment is the angle between the triangle face and the line connecting a new point to the triangle vertices. The algorithm proceeds until no more points are added. (Vosselman, 2000) proposed a slope based filtering method for separating off-terrain points from terrain points. A point is classified as a terrain point if there is no other point within a certain neighbourhood such that the height difference between the two points is larger than an allowed maximum height difference. (Wack and Wimmer, 2002) proposed a hierarchical grid-based approach for generating a DTM from laser data. They start

with a coarse grid of 9m grid width and define the raster height by selecting the lowest height from 99% of all points within the raster element. The Laplacian of Gaussian operator in combination with a weight function is utilized to detect and remove the points that are not considered to be ground points. A progressive morphological filtering method is developed by (Zhang et al., 2003) with the target to remove the non-ground measurements from LIDAR data sets. The algorithm utilizes the classical morphological opening and gradually increases the size of the structuring element. The resulting elevation differences are used to classify ground and non-ground points by applying a threshold which depends on the structuring element size. In this paper an iterative filtering approach based on the geodesic morphology operation (Lantuejoul and Maisonneuve, 1984) is proposed in order to eliminate the off-terrain points. The classical morphology operations such as erosion and dilation filter images by employing a predefined structuring element window. In geodesic morphological operations two images are involved, in contrast to the classical operations where an image and a structuring element are to be specified. A basic operation is applied to the first image and then it is forced to remain either higher or lower than the second image. The overall goal of the geodesic morphological reconstruction presented in the next section is to separate off-terrain points from terrain points. The paper is organized as follows. In Section 2 a brief introduction into morphological reconstruction based on geodesic dilation is given. Section 3 presents the overall approach for separating terrain and off-terrain points. Experimental investigations are discussed in Section 4 and some conclusions are drawn in the final section.

## 2 IMAGE RECONSTRUCTION BY MORPHOLOGICAL GEODESIC OPERATION

Morphological gray scale reconstruction based on geodesic operations employs two input images. The images are called *marker* and *mask* images. Both images must have the same size and the

mask image must have intensity values greater or equal to the marker image. In geodesic dilation the marker image is dilated by an elementary isotropic structuring element and the resulting image is forced to remain below the mask image. This means, the mask image acts as a limit for the dilated marker image. In the following the marker image is denoted by  $J$  and the mask image by  $I$ . The geodesic dilation of size 1 of the marker image  $J$  with respect to mask image  $I$  is defined as (Vincent, 1993):

$$\delta_I^{(1)}(J) = (J \oplus B) \wedge I, \quad (1)$$

In this equation,  $\wedge$  stands for the point-wise minimum between the dilated marker image and the mask image,  $J \oplus B$  is the dilation of  $J$  with the elementary isotropic structuring element  $B$ . The geodesic dilation of size  $n$  of the marker image  $J$  with respect to a mask image  $I$  is obtained by performing  $n$  successive geodesic dilations of size 1 of  $J$  with respect to  $I$ .

$$\underbrace{\delta_I^{(n)}(J) = \delta_I^{(1)}(J) \circ \delta_I^{(1)}(J) \circ \dots \circ \delta_I^{(1)}(J)}_{n\text{-times}} \quad (2)$$

Equations 1, 2 define the morphological reconstruction by geodesic dilation of the mask  $I$  from marker  $J$ . The desired reconstruction is achieved by carrying out geodesic dilations until stability is reached (Vincent, 1993). In other words, morphological reconstruction can be thought of conceptually as repeated dilations of the marker image until the contour of the marker image fits under the mask image. In this way, the peaks in the marker image spread out, or dilate. Each successive dilation operation is forced to lie underneath the mask. When further dilations do not change the marker image any more, the processing is finished. Figure 1 represents the morphological reconstruction of a

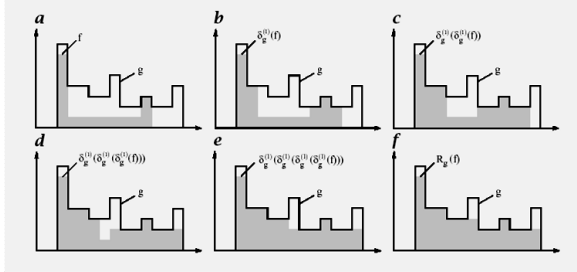


Figure 1: Morphological reconstruction using geodesic dilation; Geodesic dilation of size 5 of marker  $f$  with respect to mask  $g$  is equivalent to the reconstruction of  $g$  from  $f$  because further geodesic dilations no longer modify the result (Vincent, 1993)

1D signal  $g$  from a marker signal  $f$ . The 5-fold geodesic dilation of the marker signal with respect to the mask signal is equivalent to the reconstruction of  $g$  from  $f$  since further geodesic dilations do not modify the result anymore. In figure 1, (a) represents the 1D marker signal  $f$  and the mask signal  $g$ ; (b) to (f) show geodesic dilations of  $f$  with respect to  $g$ . Morphological image reconstruction based on geodesic dilation has some unique properties compared to basic morphology operations: (1) Two images are involved in processing, rather than one image and a structuring element. (2) The processing is repeated until stability, i.e. until the image no longer changes. (3) The procedure is based on connectivity rather than on a structuring element.

### 3 PROPOSED ALGORITHM

The proposed algorithm for generating a DTM from airborne LIDAR data is presented in figure 2. In the first step a regularly

spaced elevation grid is generated from the 3D raw data by spatial interpolation. As depicted in the figure, the segmentation of the off-terrain regions is performed in two steps: *Segmentation of regions below the ground* and *Segmentation of regions above the ground*. Obviously, in order to provide digital terrain mod-

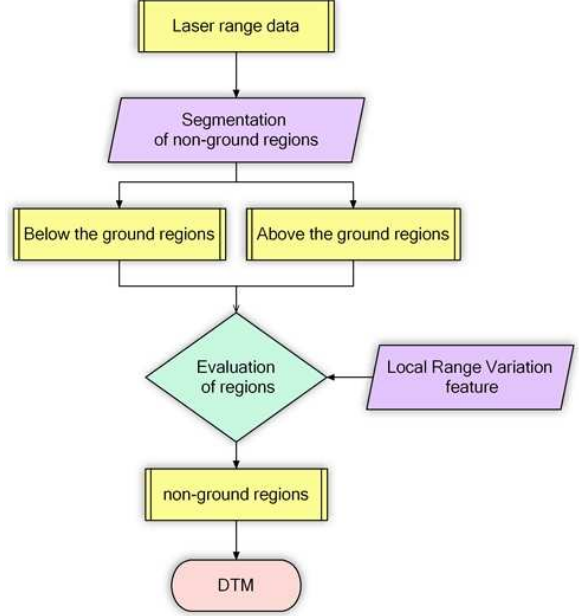


Figure 2: Generating Digital Terrain Model from airborne LIDAR data

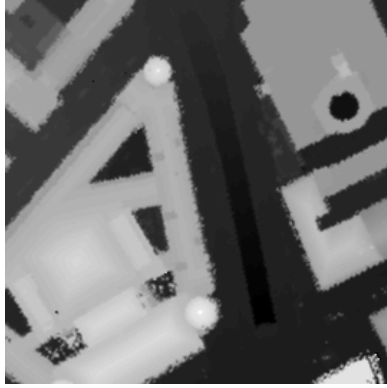
els from laser data not only the 3D regions having certain jumps above the ground are to be detected and then filtered out from the surface but also the regions having height jumps below the ground surface are to be eliminated from the DSM. Some regions such as the underground entrances, wells, swimming pools, ... can serve as examples where points in a lower height level than the ground level exist. Figure 3(a) shows an example of such regions. It shows an underground entrance in the middle of a street between some big buildings. In figure 3(b) the xyz laser data are plotted and visualized from side view. It indicates that such regions should clearly be filtered from DSM.

As explained in section 2, in the image reconstruction algorithm two data sets are involved namely *mask* and *marker* images. Since, as explained before, off-terrain regions contain surfaces above and below the ground, the segmentation process performs in two steps. Depending on the region to be filtered different *mask* and *marker* images should be created. In the first segmentation step regions above the terrain are filtered using the *mask* image which is equal to the original image ( $LR$ ) whereas in the second segmentation step the regions below the terrain are filtered using the *mask* image which is equal to the complement of the original image ( $LR'$ ). In fact by complementing or inverting of the image we are aiming to convert regions below the terrain to the above ones. Equation 3 shows how the complemented image ( $LR'$ ) is produced by subtracting the  $LR$  image from the *maximum* value of it.

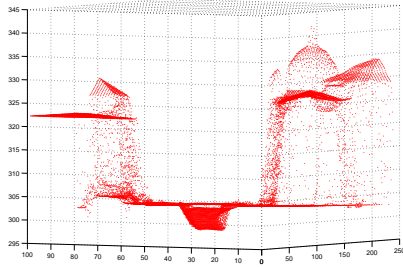
$$LR' = \max(LR) - LR \quad (3)$$

The *Marker* image is produced as an image with same size as the *mask* image and its gray values equal to the minimum gray value of mask image. Equation 4 is used for filtering of the regions above the terrain and equation 5 is employed for filtering of the regions below the terrain.

$$Marker = \min(LR) * \text{ones}(\text{size}(LR)) \quad (4)$$



(a) LIDAR range data



(b) profile of the underground entrance and surrounding

Figure 3: Underground entrance - Stuttgart

$$Marker' = \text{minimum}(LR') * \text{ones}(\text{size}(LR')) \quad (5)$$

Figure 4 shows the procedure of segmentation of off-terrain pixels based on the morphological reconstruction algorithm.

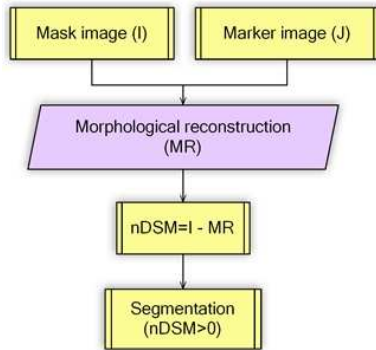


Figure 4: Segmentation by morphological geodesic dilation

Observing equation 2, morphological geodesic dilation proceeds for each segmentation step until stability reached. In this phase most of the potential off-terrain regions will be filtered out by the image reconstruction algorithm.

As illustrated in figure 1, geodesic reconstruction algorithm filters the objects are higher than their surrounding in the image. That means all the pixels on the boundary of object must have bigger value comparing to the pixels outside next to the object. In LIDAR range images the desired 3D objects (such as buildings and trees) to be filtered are often higher than their neighborhood. In the suburban hilly regions it happens occasionally that the spacious buildings are situated on the steep terrain. As instance a sample of such buildings is presented in Figure 5. In this region, as shown, the road next to the building on the left hand side has bigger height (327.0 m) comparing to a part of the building on



Figure 5: Spacious building block - special case; Height value on the roof in one side (right) is less than the height of the road next to it (left)

the right hand side (322.6 m). This means the building is not situated completely higher than its neighborhood pixels. In this case the morphology reconstruction algorithm is not able to filter such objects in one step. Therefore an approach is proposed to filter iteratively individual parts of the object. In this method in the first iteration the inner parts of the object which are higher than the neighborhood are filtered. The filtered regions are then removed from the original image and produces new *mask*. In this *mask* image usually the part of the object that was in the lower height level, will be isolated and disconnected from the original object. Therefore in the next reconstruction process this part will be filtered as well (see figure 8).

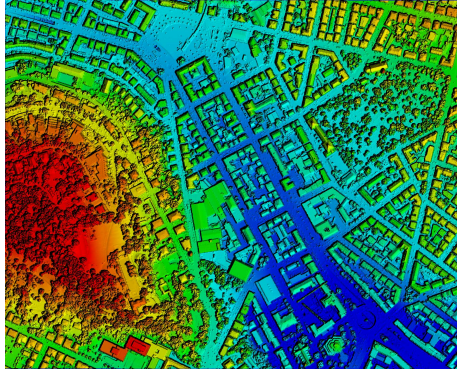
After performing image reconstruction, the reconstructed image (*ImRec*) is subtracted from the *mask* image to generate an image very similar to *TopHat* or *nDSM* image (in contrast to the classical morphology operation):

$$nDSM = LR - ImRec, \quad (6)$$

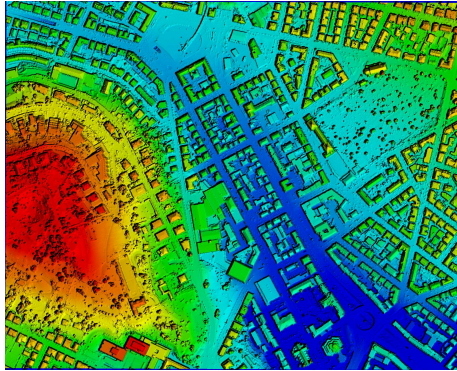
As illustrated in figure 4 the segmentation process is performed by consideration of the pixels having gray levels bigger than *zero*. This is an advantage of geodesic morphology comparing to the classical morphology operation. In classical operations one should always care about selecting a proper threshold value for segmentation while in geodesic operations this value is always zero. In geodesic operations the background regions are smoothly eliminated and the pixels in the neighborhood of the objects are always zero.

After thresholding the regions are created using connected components analysis based on connectivity of the segmented pixels. The produced regions are evaluated by means of the *Local Range Variation (LRV)* feature. This feature highlights the height jumps in the image. The *LRV* feature is created by subtracting the *maximum* and *minimum* values in every  $3 \times 3$  window over the image. All the boundary pixels of the detected regions are evaluated by the *LRV* descriptor. The regions having height jumps above a certain threshold on their boundaries will be evaluated as off-terrain regions. In practice the *LRV* values of each boundary region are extracted. If the majority (here 90 percent) of the *LRV* values are above the threshold (here 0.5m), the region will be classified as off-terrain and its location will be eliminated from the original data set to produce a new *mask* image. Hence the new *mask* image is the original image without the detected off-terrain regions. This procedure is iterated until all off-terrain areas are filtered. Usually in very rough hilly residential areas the iteration number does not exceed 5. After eliminating all off-terrain regions from the original image the produced gaps are filled by means of a spatial interpolation procedure.

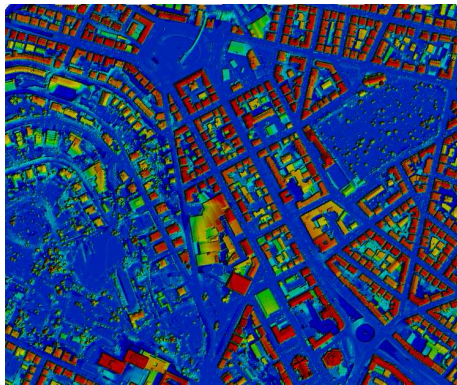
The procedure to separate off-terrain regions from the LIDAR image is summarized as following:



(a) First Pulse LIDAR data



(b) Last Pulse LIDAR data



(c) Normalized DSM produced in final step

Figure 6: Airborne LIDAR data and some processing results (area=  $1 \text{ km}^2$ , min height=204.5 m, max height=407.5 m)

1. Create *mask* image
2. Create *marker* image
3. Perform image reconstruction using equations 1 and 2
4. Calculate  $nDSM$  using equation 6
5. Binarize using  $BW = (nDSM > 0)$
6. Generate regions using connected components analysis from binary image ( $BW$ )
7. Evaluate regions using  $LRV$  feature and extract off-terrain regions
8. Remove off-terrain regions from *mask* image and produce new *mask*



Figure 7: Local Range Variation ( $LRV$ ) image which mainly highlights height jumps in range image

9. Go to step 3 and perform image reconstruction by means of new *mask* image
10. procedure continued until no more change happens between new and old *mask* images

Based on the algorithm for segmentation of the regions below and above the terrain the *mask* and *marker* images vary in step 1 and 2. As explained before the *mask* image to segment regions above the terrain is equal to the original data ( $LR$ ) and its *marker* is produced using equation 4. Segmentation of the regions below the terrain is performed by the *mask* and *marker* created by equations 3 and 5.

#### 4 EXPERIMENTAL INVESTIGATION

The concept for detecting and eliminating the non-ground regions from the digital surface model is tested with a LIDAR data set which shows a suburban area (figures 6(a) and 6(b)). A  $1 \text{ km}^2$  hilly residential area with maximum height difference about 203 m is selected for experiment. The area contains different 3D objects placed over the undulated terrain such as very dense vegetation regions as well as spacious building blocks.

The data is recorded with TopScan's Laser Terrain Mapper systems, (TopScan, 2007) from the city of Stuttgart, Germany. A regularly spaced elevation grid is generated by means of spatial interpolation of the raw 3D points. The average density of the irregularly recorded 3D points is close to 4 per square meter; a 0.5 meter lattice spacing is chosen as elevation grid. In previous section is outlined how the off-terrain regions are classified in the iterative approach.

Figure 6(c) illustrates the normalized DSM generated by the reconstruction method. This image produced by subtracting the original image ( $LR$ ) from the morphological reconstructed image ( $ImRec$ ) as shown in equation 6. The detection process is then performed using simple thresholding on the  $nDSM$  image. The foreground pixels in this step are analyzed in order to create regions by means of connected components analysis. All the regions are now evaluated by  $LRV$  (figure 7). As explained the off-terrain regions are iteratively filtered using different *mask* and *marker* images which are generated sequentially in the process. Figure 8(a) highlights the regions below the terrain detected by the algorithm. We called them below the terrain regions but in fact they are the regions having a certain height jump (here 0.5 m) comparing to their neighborhoods. The above the terrain regions

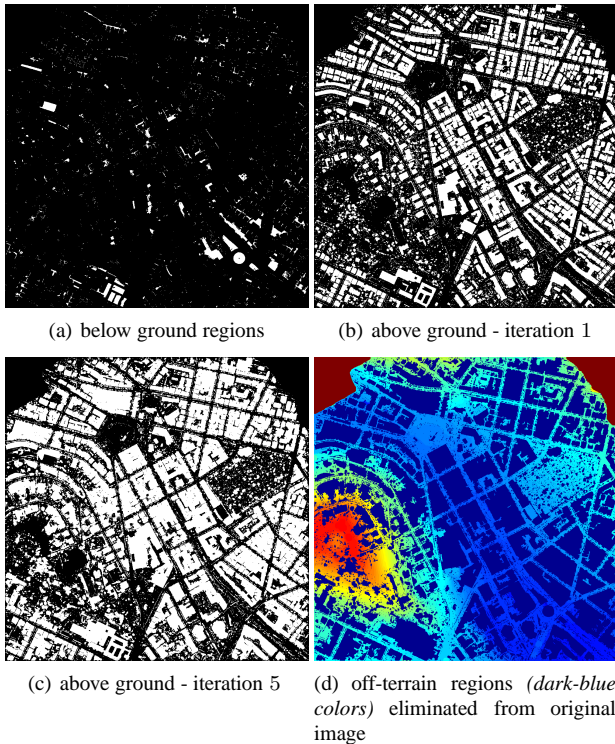


Figure 8: Off-terrain regions segmented using morphological geodesic dilation and evaluated by LRV feature

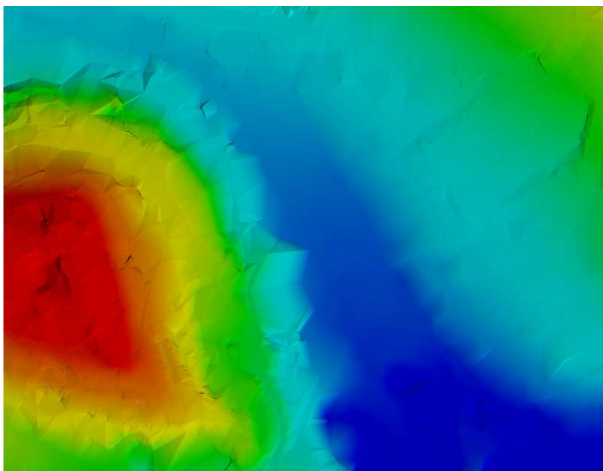


Figure 9: Produced DTM after interpolation of the gaps

detected after first iteration is shown in figure 8(b). The spacious building which was discussed before is visible at the middle of the image. The result illustrates that the complete parts of the building is not filtered yet. Figure 8(c) displays all the above the terrain regions detected and finally all off-terrain regions, including below and above the ground regions, are highlighted in figure 8(d). Finally a surface model is generated from the LIDAR data after removing all non-ground points, i.e. a DTM, is visualized in Figure 9.

## 5 CONCLUSIONS

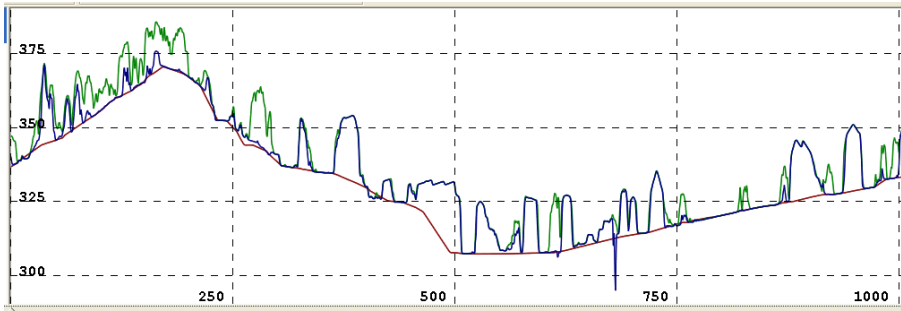
Figure 8(d) shows that almost all the eye-catching off-terrain regions have been eliminated. These regions mainly represent buildings and vegetation areas. None of the buildings is visible any more and also the vegetation has virtually disappeared. Shape and size of the objects is obviously irrelevant in our approach. Large

buildings as well as small ones, elongated buildings as well as shortened ones and high buildings as well as low ones have been properly eliminated.

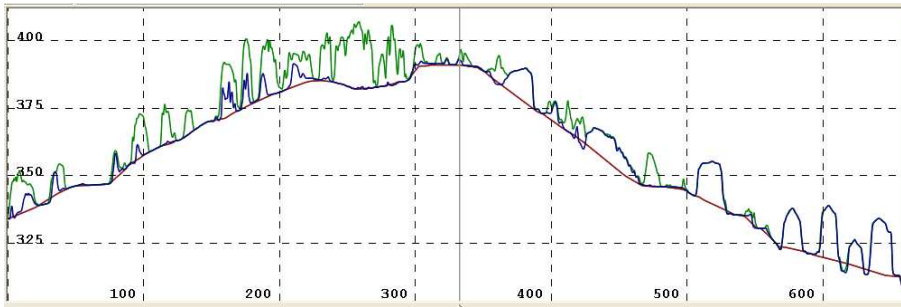
In addition to visually evaluating the results, three profiles have been provided along the image and are plotted in figure 10. The first pulse LIDAR values are displayed in green, the last pulse in red. Regions above the ground as well as surfaces below the ground can be seen in sample areas. The profiles show that the algorithm could properly detect and eliminate the off-terrain regions from original data set.

## REFERENCES

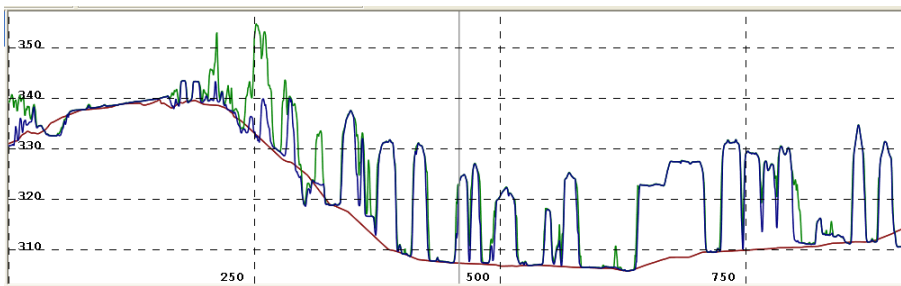
- Arefi, H. and M. Hahn, 2005. A morphological reconstruction algorithm for separating off-terrain points from terrain points in laser scanning data. Proceedings of the ISPRS Workshop Laser scanning.
- Axelsson, P., 2000. DEM generation from laser scanner data using adaptive tin models. International Archives of Photogrammetry and Remote Sensing.
- Kilian J., N. Haala and M. Englich, 1996. Capture and evaluation of airborne laser scanner data. International Archives of Photogrammetry and Remote Sensing.
- Kraus K. and N. Pfeifer, 1998. Determination of terrain models in wooded areas with airborne laser scanner data. ISPRS Journal of Photogrammetry and Remote Sensing 53, pp. 193–203.
- Lantuejoul Ch. and F. Maisonneuve, 1984. Geodesic methods in image analysis. Pattern recognition 17, pp. 117–187.
- Sithole, G. and G. Vosselman, 2003. Report: Isprs comparison of filters. ISPRS Commission III, Working Group 3.
- TopScan, 2007. <http://www.topscan.de/>, visited february 2007.
- Vincent, L., 1993. Morphological grayscale reconstruction in image analysis: Applications and efficient algorithms. IEEE Transactions on Image Processing 2, pp. 176–201.
- Vosselman, G., 2000. Slope based filtering of laser altimetry data. International Archives of Photogrammetry and Remote Sensing XXXIII, B3, pp. 935–942.
- Wack R. and A. Wimmer, 2002. Digital terrain models from airborne laser scanner data - a grid based approach. International Archives of Photogrammetry and Remote Sensing.
- Zhang K., S. Chen, D. Whitman, M. Shyu, J. Yan and C. Zhang, 2003. A progressive morphological filter for removing non-ground measurements from airborne lidar data. IEEE Trans. on Geoscience and Remote Sensing 41, Issue 4, pp. 872–882.



(a) Profile Nr.1; from upper-left corner to lower-right corner



(b) Profile Nr.2; from left to right at the middle of image



(c) Profile Nr.3; from lower-left corner to upper-right corner

Figure 10: Sample profiles along the image; (*green=first pulse*, *blue=last pulse* and *red=DTM*)